

# Finite-difference modeling of borehole induction data in the presence of 3D electrical conductivity anisotropy using coupled scattered potentials

Junsheng Hou<sup>\*</sup>, and Carlos Torres-Verdín, The University of Texas at Austin, USA

## Summary

We describe a novel finite-difference (FD) forward modeling method to simulate borehole electromagnetic (EM) fields in arbitrary three-dimensional (3D) electrically anisotropic media. This novel simulation method is based on the boundary-value problem of coupled scattered vector-scalar potentials. We solve the ensuing boundary-value problem with a central FD approximation on a Yee's staggered grid. Such an approximation produces a linear system of equations that is sparse and complex non-symmetrical. The final linear system is iteratively solved using a Krylov subspace solver—the improved stabilized complex bi-conjugate gradient method (BICGSTAB (L)). This solver significantly accelerates the converge rate compared to conventional conjugate gradient, the bi-conjugate gradient (BICG) methods and BICGSTAB. In addition, we make use of an efficient optimal grid refinement strategy that considerably reduces memory requirements without sacrifice of accuracy. We provide examples of the numerical simulation of borehole EM induction instruments to assess the validity, efficiency, and accuracy of the new numerical formulation. All numerical examples considered in the benchmark study indicate that the scattered potential FD method successfully competes with alternative finite-difference methods used to simulate borehole EM logging responses in the presence of 3D inhomogeneous anisotropic media.

## Introduction

Theoretical analyses and numerical experiments show that the potential finite-difference (FD) formulation has obvious advantages over conventional electromagnetic (EM) field FD formulations (see, for instance, LaBrecque, 1999, Haber et al., 2000 and 2001, Newman and Alumbaugh, 2002, Hou and Torres-Verdín, 2003, and Weiss and Newman, 2003). The potential formulation is becoming a popular numerical technique for FD modeling of EM fields in complex three-dimensional (3D) anisotropic media.

During the last year's SEG annual meeting the authors (Hou and Torres-Verdín, 2003) presented the research results concerning FD modeling of EM fields in a 3D anisotropic medium with the coupled total potential formulation. We have subsequently refined our FD method, including the algorithm and code in several ways. First, based on some advantages of the scattered field formulations over the total field formulation, we implemented a scattered coupled potential formulation to simulate subsurface EM diffusion and propagation. Second, because of the irregular oscillating

behavior of the bi-conjugate gradient (BICG) solver for non-uniform grids, the BICG was replaced by the improved stabilized complex bi-conjugate gradient method (BICGSTAB (L)) (Sleijpen and Fokkema, 1993) with preconditioning. Finally, we implemented the optimal grid method described by Davydycheva et al., 2003 for spatial gridding in conjunction with the scattered potential formulation.

## Theory

Assuming a time-harmonic variation of the form  $e^{i\omega t}$  where  $i = \sqrt{-1}$ , the frequency-domain Maxwell's equations for the scattered EM field in arbitrary 3D inhomogeneous anisotropic media can be expressed as

$$\nabla \times \mathbf{E}_s = -i\omega \mathbf{m}_0 \cdot \mathbf{H}_s, \quad (1)$$

$$\nabla \times \mathbf{H}_s = \mathbf{s}' \mathbf{E}_s + \mathbf{J}_s, \quad (2)$$

and

$$\nabla \cdot \mathbf{H}_s = 0. \quad (3)$$

In these equations  $\mathbf{s}' = \mathbf{s} + i\omega \mathbf{e}$  is a complex conductivity tensor,  $\mathbf{s}$  is an Ohmic conductivity tensor,  $\mathbf{e}$  is dielectric permittivity,  $\mathbf{m}_0$  is the free-space magnetic permeability, and  $\omega$  is the angular frequency of EM fields. The scattered electric and magnetic fields are denoted by  $\mathbf{E}_s$  and  $\mathbf{H}_s$ , respectively, and  $\mathbf{J}_s$  is an equivalent source current density defined by

$$\mathbf{J}_s = (\mathbf{s}' - \mathbf{s}'_b) \cdot \mathbf{E}_b, \quad (4)$$

where  $\mathbf{s}'_b$  is the complex conductivity of the background medium and  $\mathbf{E}_b$  is the background electric field. The background medium may be a full space, a 1D layered formation, or some other basic model in which the background fields can be easily calculated. In the following numerical examples, the background medium is assumed to be an isotropic and homogeneous full space with physical properties equal to those of the rock formation at the source location.

From the scattered Maxwell's equations, we can obtain the following second-order partial differential equations (PDEs) governing the coupled scattered vector-scalar potentials

$$\nabla^2 \mathbf{A}_s - i\omega \mathbf{m}_0 \mathbf{s}' \mathbf{A}_s - \mathbf{s}' \cdot \nabla V_s = -\mathbf{J}_s, \quad (5)$$

and

$$i\omega \mathbf{m}_0 \nabla \cdot (\mathbf{s}' \mathbf{A}_s) + \nabla \cdot (\mathbf{s}' \cdot \nabla V_s) = \nabla \cdot \mathbf{J}_s, \quad (6)$$

where the vector  $\mathbf{A}_s$  is the scattered magnetic vector potential

that satisfies the Coulomb gauge, and the scalar  $V_s$  is the scattered electric scalar potential. In the scattered potential formulation, we consider homogeneous Dirichlet boundary conditions. Equations (5) and (6) and the boundary conditions define the boundary-value problem for the scattered potentials.

The corresponding relationships between scattered EM fields and coupled scattered potentials are

$$\mathbf{E}_s = -i\omega\mu_0 \cdot \mathbf{A}_s - \nabla V_s, \quad (7)$$

and

$$\mathbf{H}_s = \nabla \times \mathbf{A}_s. \quad (8)$$

It follows that if the scalar and vector potentials are calculated then the scattered EM fields may be obtained directly from equations (7) and (8). Finally, the total EM fields are determined from the expressions  $\mathbf{E}_s + \mathbf{E}_b$  and  $\mathbf{H}_s + \mathbf{H}_b$ , where  $\mathbf{H}_b$  is the background magnetic field. Next we approach the numerical solution of the boundary-value problem for the coupled scattered potentials using the FD method on a Yee's staggered grid (Yee, 1966).

We make use of a spatial gridding method similar to that of the total potential formulation. Finally, we obtain the following matrix equation

$$\mathbf{A} \mathbf{x} = \mathbf{B}, \quad (9)$$

where  $\mathbf{A} = (a_{ij})_{N \times N}$  is a non-symmetric complex matrix with only limited non-zero elements in every row, and  $N$  is the number of unknowns. The linear system matrix  $\mathbf{A}$  is large and sparse; its entries mainly depend on both the grid spacing and the spatial distribution of electrical conductivity. In equation (9),  $\mathbf{x}$  is the vector of unknown complex values of the scattered potentials at the grid nodes, and  $\mathbf{B}$  is the right-hand side vector containing source terms associated with the boundary conditions.

In our total potential formulation, we solve equation (9) using the complex BICG with precondition. Although BICG is an ideal linear solver for many practical problems, it has a few obvious disadvantages. For instance, the BICG often exhibits irregular oscillating convergence behavior in the residual norm, which may decrease the speed of convergence. To further accelerate the convergence rate of the linear system (9), we use the BICGSTAB (L) solver, which overcomes these shortcomings of BICG and BICGSTAB. In addition, the accuracy and computation time of the FD method primarily depend on the spatial gridding. To further reduce computation times we have incorporated an optimal FD grid refinement to the new potential formulation thereby considerably reducing the total number of nodes without sacrificing accuracy.

## Numerical examples

We consider two canonical models of borehole EM induction to validate and benchmark the FD code and to demonstrate its applicability to 3D modeling problems. The numerical examples assume a multi-component induction-logging instrument. This instrument consists of one transmitting and one receiving coil separated by a distance of 1m. The coils can be oriented in the x, y, or z directions. Electromagnetic measurements are denoted as  $F_{pq} = \text{Re}(F_{pq}) + i \text{Im}(F_{pq})$ , where  $\text{Re}(F_{pq})$  is the real part,  $\text{Im}(F_{pq})$  is the imaginary part, the subscript  $p$  indicates the moment orientation of the transmitter, and the subscript  $q$  indicates the orientation of the receiver. For instance,  $\text{Im}(H_{zz})$  and  $\text{Re}(H_{zz})$  are the imaginary and real parts of the vertical magnetic field  $H_{zz}$ , respectively, produced by a z-directed magnetic dipole transmitter. The spatial grid used to simulate the following results consists of 24 nodes in the x and y directions, respectively, and 92 nodes in the z-direction. Figure 1 shows the first model (Model-1). It consists of a 1D anisotropic layered formation dipping at an angle of 60 degrees without the presence of a borehole. The corresponding simulation results obtained for a probing frequency of 200 kHz are shown in Figures 2 through 5. Figure 6 shows the second model (Model-2). It consists of a 1D anisotropic layered formation dipping at an angle of 60 degrees in the presence of a borehole (a full 3D model). The corresponding EM numerical results at 200 kHz are shown in Figures 7 through 10. Numerical results are compared to the total potential solution, thereby indicating an excellent agreement between the two solutions.

## Discussion and Conclusions

The novel FD modeling algorithm based on scattered potentials provides higher accuracy and faster computational speed than a total potential. For example, it only takes an average of less than two minutes of CPU time to simulate monochromatic EM fields for one depth point on a Pentium® 4 (2.0 GHz) personal computer for the above models. Moreover, simulation problems can be accurately and efficiently solved in the presence of high contrasts in electrical conductivity. The same algorithm can be used to simulate EM diffusion and propagation over a wide frequency band. Simulation exercises considered in this paper include non-conventional EM field components such as  $H_{zx}$  and  $E_{zy}$  besides  $H_{zz}$ ,  $H_{xx}$ , and  $H_{yy}$ . The latter components could be used as indicators formation dipping and anisotropy.

## Acknowledgements

UT Austin's Research Consortium on Formation Evaluation, jointly sponsored by Baker Atlas, Halliburton, Schlumberger, Shell International E&P, Anadarko Petroleum Corporation,

ConocoPhillips, ExxonMobil, and TOTAL, provided funding for the work reported in this paper.

**References**

Davydycheva, S., Druskin, V., and Habashy T., 2003, An efficient finite-difference scheme for electromagnetic logging in 3D anisotropic inhomogeneous media: *Geophysics*, 68, 1525-1536.

Haber, E., Ascher, U. M., and Oldenburg, D. W., 2000, Fast simulation of 3D electromagnetic problems using potentials: *J. Comput. Phys.*, 163, 150-171.

Haber, E. and Ascher, U. M., 2001, Fast finite volume simulation of 3D electromagnetic problems with highly discontinuous coefficients: *SIAM J. Sci. Comput.*, 22, 1943-1961.

Hou, J. and Torres-Verdin, C., 2003, Finite-difference modeling of EM fields using coupled potentials in 3D anisotropic media: application to borehole logging: 73<sup>rd</sup> Ann. Internat. Mtg., Soc. Expl. Geophys., Expanded Abstracts, 522-525.

LaBrecque, D. J., 1999, Finite difference modeling of 3-D EM fields with scalar and vector potentials, in Oritaglio, M., and Spies, B., Eds., *Three-dimensional electromagnetics*: Soc. Expl. Geophys, 146-160.

Newman, G. A. and Alumbaugh, D. L., 2002, Three-dimensional induction logging problems, Part 2: A finite difference solution: *Geophysics*, 67, 484-491.

Sleijpen, G. L. G. and Fokkema, D. R., 1993, BICGSTAB (L) for linear equations involving unsymmetric matrices with complex spectrum: *ETNA*, 1, 11-32.

Weiss, C. J. and Newman, G. A., 2003, Electromagnetic induction in a generalized 3D anisotropic earth, Part 2: The LIN preconditioner: *Geophysics*, 68, 922-930.

Yee, K.S., 1966, Numerical solution of initial boundary value problems involving Maxwell's equations in isotropic media: *IEEE Trans. Antennas Prop.*, AP-14, 302-307.

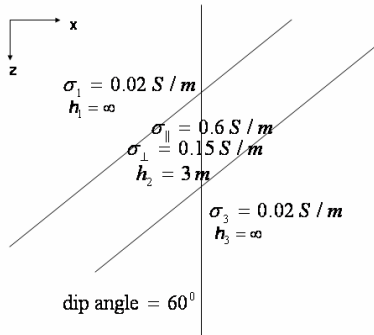


**Fig. 1:** An anisotropic layered formation dipping at an angle of 60 degrees without the presence of a borehole (model-1).

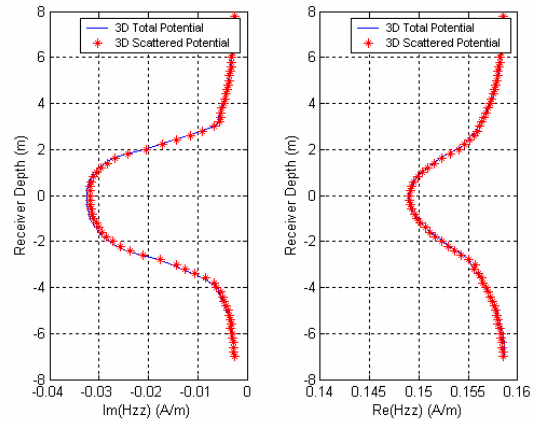


**Fig. 2:** Comparisons of Hzz with the scattered and total potentials for model-1. The probing frequency is 200 kHz.

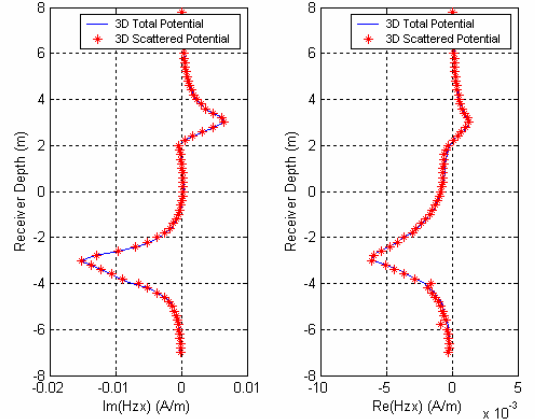


**Fig. 3:** Comparisons of Hxz with the scattered and total potentials for model-1. The probing frequency is 200 kHz.

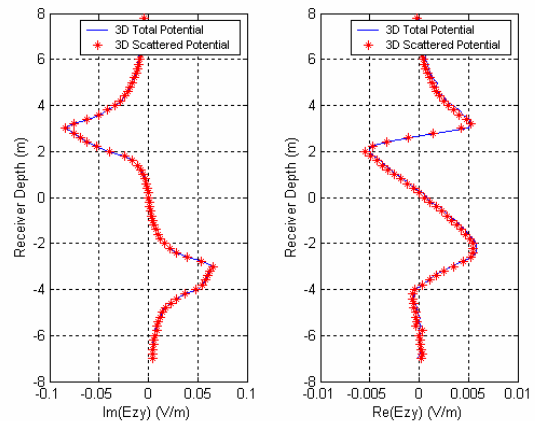


**Fig. 4:** Comparisons of Ezy with the scattered and total potentials for model-1. The probing frequency is 200 kHz.

3D FD modeling of borehole induction data with scattered potentials in the presence of conductivity anisotropy

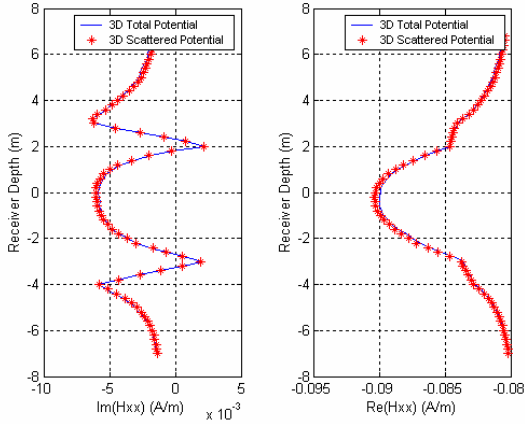


Fig. 5: Comparisons of  $H_{xx}$  with the scattered and total potentials for model-1. The probing frequency is 200 kHz.

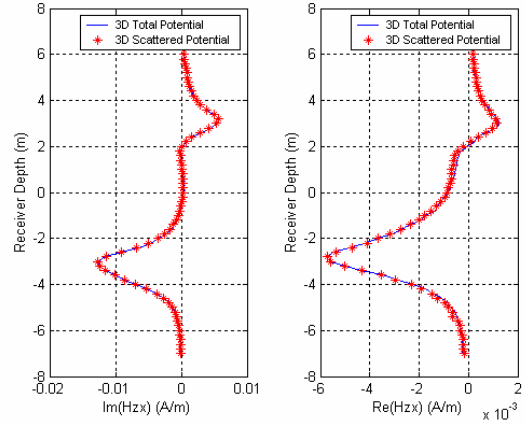


Fig. 8: Comparisons of  $H_{xz}$  with the scattered and total potentials for model-2. The probing frequency is 200 kHz.

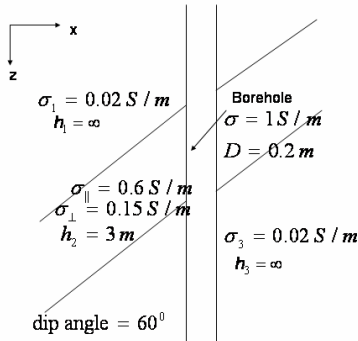


Fig. 6: An anisotropic layered formation dipping at an angle of 60 degrees in the presence of a borehole (model-2).

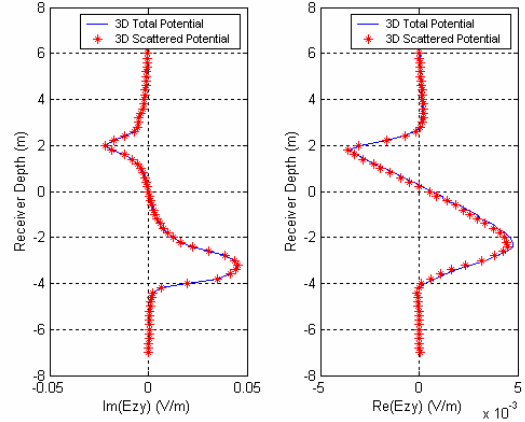


Fig. 9: Comparisons of  $E_{zy}$  with the scattered and total potentials for model-2. The probing frequency is 200 kHz.

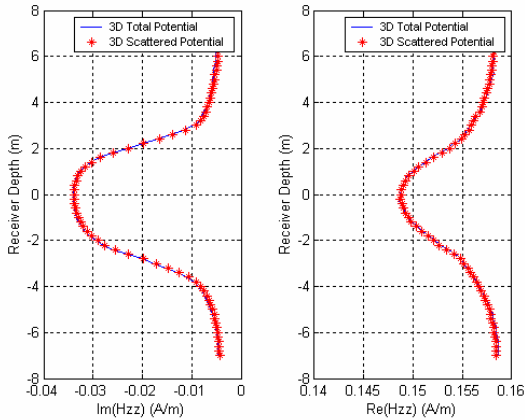


Fig. 7: Comparisons of  $H_{zz}$  with the scattered and total potentials for model-2. The probing frequency is 200 kHz.

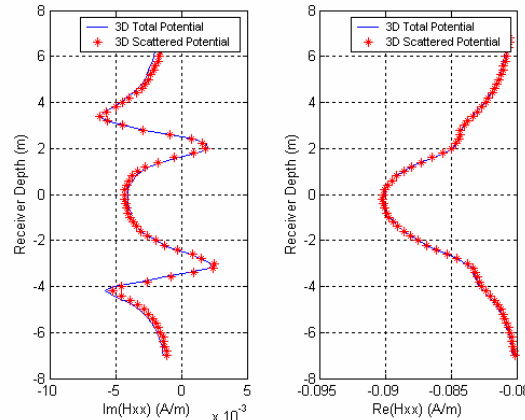


Fig. 10: Comparisons of  $H_{xx}$  with the scattered and total potentials for model-2. The probing frequency is 200 kHz.